Applications and Development of Agrometeorology
Chapter 6 Interactions Among Atmosphere, Soil, and Vegetation
69 - 92, 2001

Chapter 6 Interactions Among Atmosphere, Soil, and Vegetation

Wen-Yih Sun
Department of Earth and Atmospheric Sciences, Purdue University,
West Lafayette, IN 47905, U.S.A.

ABSTRACT ---------- 70
1. INTRODUCTION ---------- 70
2. ONE-DIMENSIONAL BASIC EQUATIONS ---------- 72
3. RESULTS ---------- 77
4. SUMMARY ---------- 87
5.REFERENCES ---------- 88
摘 要 ---------- 91

Chapter 6 Interactions Among Atmosphere, Soil, and Vegetation

Wen-Yih Sun

Department of Earth and Atmospheric Sciences, Purdue University,
West Lafayette, IN 47905, U.S.A.

ABSTRACT

Fundamental equations of the atmosphere-land surface interactions are presented. Based upon those equations, we have developed the atmospheric and land-surface models at Purdue University. The numerical results show the models are capable of reproducing the major features of observations. Models also help us to understand the physical processes involved in atmosphere, soil and vegetation. However, it is obvious that more observational data should be collected and more scientists in different disciplines should work together to study the mechanisms at and near the land surface, which is crucial before a comprehensive model can be developed to predict the change of climate, water resources, and ecology accurately.

Key words: Basic equations, Potential temperature, Mixing ratio, Richards' equation, Darcy-buckingham equation, Matric potential, Hydraulic conductivity, Resistance, Minimum stomatal resistance, Height of canopy, Leaf area index (LAI), PBL, Canopy coverage, Wilting point, Field capacity, Surface energy budget, Surface moisture budget, Stand alone model, Soil texture, Soil moisture.

1. INTRODUCTION

It is well know that the growth of vegetation strongly depends upon temperature, radiation, and soil moisture. Soil moisture is controlled by precipitation, runoff, and the surface moisture flux, which includes evaporation from bare ground and vegetation.

On the other hand, vegetation and soil moisture also influence the surface heat and moisture fluxes as well as the local and regional climate and hydrology. Meanwhile, vegetation can prevent soil erosion and reduce air pollution, and the occurrence of drought and flood. Therefore, the interactions among the atmosphere, soil, and vegetation are crucial to agriculture, weather, climate, air pollution control, and water resources (Manabe 1969; Bhumralkar 1975; Dickinson 1984). Figure 1 (Dickinson *et al.*, 1993) is a schematic diagram of the atmosphere-land surface interaction. It requires scientists in many areas, such as soil science, atmospheric sciences, hydrology, agriculture, biosphere to work together to solve this important problems. Unfortunately, this area has been ignored in many countries, including Taiwan.

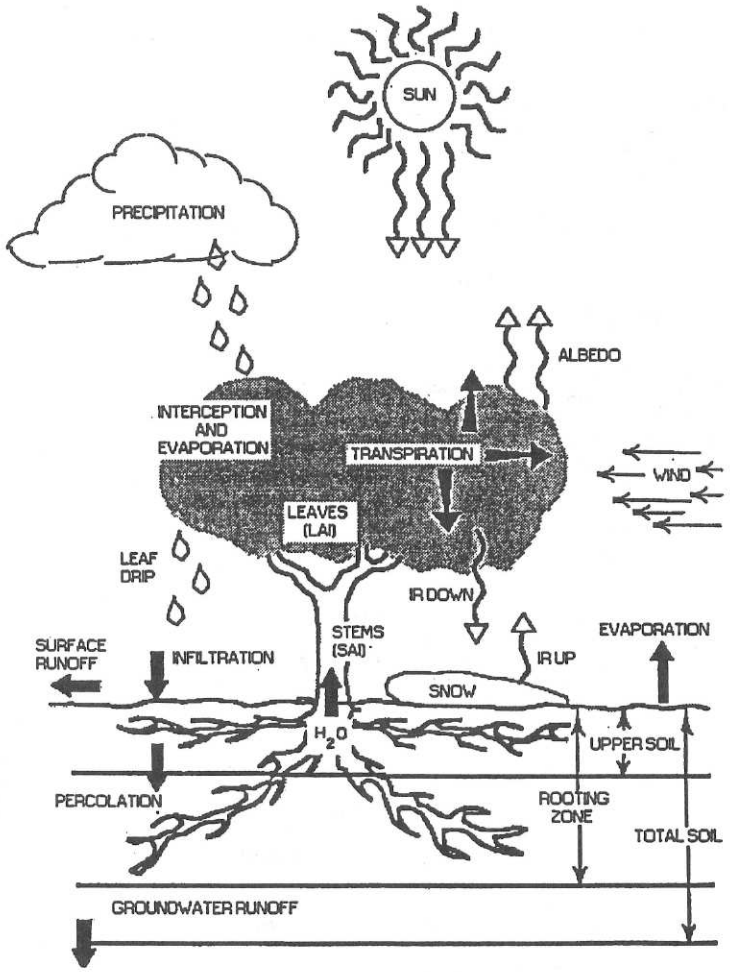


Fig. 1 (after Dickinson et *al.*, 1993)

The soil temperature, evaporation rate, humidity, the property and distribution of soil and vegetation are not included in the routine meteorological observations. They have been collected only by a few special field experiments around the world. But the surface moisture and heat fluxes are required in a numerical weather prediction model. Therefore, scientists (Philip, 1957; Deardorff, 1977, 1978; Clapp and Hornberger, 1978; Beljaars *et al.*, 1996; Wu and Sun, 1990a, b; Bosilovich and Sun, 1995; and others) have developed various mathematical models to study the physical mechanisms and predict the fluxes at surface based on the conservations of momentum, energy, and water substances. Hence, my students and I have been working on the land-surface package, as a component of the 3-dimensional Purdue Regional Model (PRM; Sun and Chern, 1993, 1994; Chern, 1994, Haines *et al.*, 1997, etc).

The basic equations and model set up will be discussed in the next section. The modeled results and observation, as well as sensitivity test of soil wetness and vegetation will be discussed in Section 3.

2. ONE-DIMENSIONAL BASIC EQUATIONS

The model includes equations of the motion in the atmosphere, the equations at the atmosphere-vegetation-soil interface, and the equation of heat and water substances inside the soil.

2a: Equations in the atmospheric boundary layer

The equations in the one-dimensional atmospheric model are

$$\frac{\partial U}{\partial t} = f(V - V_g) - \frac{\partial \overline{uw}}{\partial z} \qquad (a.1)$$

$$\frac{\partial V}{\partial t} = -f(U - U_g) - \frac{\partial \overline{vw}}{\partial z} \qquad (a.2)$$

$$\frac{\partial \Theta_e}{\partial t} = -\frac{\partial \overline{w\theta_e}}{\partial z} - W\frac{\partial \Theta_e}{\partial z} - \frac{1}{\rho c_p}\frac{\Theta}{T}\frac{\partial R_{net}}{\partial z} \qquad (a\text{-}3)$$

$$\frac{\partial Q_w}{\partial t} = -\frac{\partial \overline{wq_w}}{\partial z} - W\frac{\partial Q_w}{\partial z} \qquad \text{(a. 4)}$$

where (U, V, W) and (u, v, w) are mean and fluctuating velocity vectors in x(eastward), y(northward), z(vertical) directions. Θ_e and θ_e are the mean and fluctuating equivalent potential temperature ($\Theta_e = \Theta + \frac{L_v}{c_p}\frac{\Theta}{T}Q$). Q_w and q_w are the mean and fluctuating water substance, where $Q_w = Q + Q_c$ and Q is mixing ratio and Q_c is cloud water content. U_g and V_g are geostrophic wind along x and y components, respectively. R_{net} is the net radiative flux. In order to solve (1)-(4), Wu and Sun (1990a, b) and Sun (1993a, b) proposed to combine the turbulent kinetic energy (TKE) ($E = 0.5(u^2 + v^2 + w^2)$) equation and K-theory to calculate the turbulence fields:

$$\frac{\partial \bar{E}}{\partial t} = -2(\overline{uw}\frac{\partial U}{\partial z} + \overline{vw}\frac{\partial V}{\partial z}) - \frac{\partial}{\partial z}\left[\overline{w(E + p/\rho)}\right] + \frac{g}{\Theta_o}\overline{w\theta} - \varepsilon \qquad \text{(a. 5)}$$

$$\overline{uw} = -\kappa_m(\frac{\partial U}{\partial z}) \qquad \text{(a. 6)}$$

$$\overline{vw} = -\kappa_m(\frac{\partial V}{\partial z}) \qquad \text{(a. 7)}$$

$$\overline{w\theta_e} = -\kappa_h(\frac{\partial \Theta_e}{\partial z} - r_c) \qquad \text{(a. 8)}$$

$$\overline{wq_w} = -\kappa_h(\frac{\partial Q_w}{\partial z}) \qquad \text{(a. 9)}$$

The eddy coefficients κ_m and κ_T ($m^2 s^{-1}$), transport term $\overline{[w(E + \frac{p}{\rho})]}$, and dissipation ε are parameterized according to Sun (1989, 1993a, b).

2b: Equations of Land-Surface

The one-dimensional conservation equations for temperature and soil moisture are

$$\frac{\partial T}{\partial t} = -\frac{1}{C_h}\frac{\partial Q_T}{\partial z} + \frac{S_T}{C_h} \qquad \text{(b. 1)}$$

$$\frac{\partial w}{\partial t} = -\frac{\partial Q_w}{\partial z} + S_w \text{(Richards' equation)} \qquad \text{(b. 2)}$$

where T is soil temperature, C_h is volumetric soil heat capacity, w is volumetric soil water content, and S_T and S_w are sink terms. The vertical heat flux Q_T obeys

$$Q_T = -K_T \frac{\partial T}{\partial z} \qquad \text{(b. 3)}$$

where K_T is thermal conductivity. The vertical soil water flux Q_w obeys

$$Q_w = K\left(1 - \frac{\partial \psi_w}{\partial z}\right) \text{ (Darcy-Buckingham equation)} \qquad \text{(b. 4)}$$

In the absence of any pressure head, the effects of gravity on viscous vertical flow of water are represented by hydraulic conductivity K. The present of any pressure head, or suction, is presented by the moisture or matrix potential ψ_w, Basically, ψ_w equals the work required to extract water from the soil against capillary (surface tension) and absorption forces. When the soil is saturated ψ_w has a minimum value, but not all air space will be filled with water. (here z is positive above the surface, but z is positive beneath surface in hydrology. Hence, we obtain

$$\frac{\partial w}{\partial t} = \frac{\partial}{\partial z}\left(K\frac{\partial \Psi_w}{\partial z}\right) - \frac{\partial K}{\partial z} + S_W \qquad \text{(b. 5)}$$

Following Clapp-Hornberger (1978), soil hydraulic property functions can be defined

$$w = w_s\left(\frac{\psi_w}{\psi_s}\right)^{-\lambda}$$
$$\frac{K}{K_s} = \left(\frac{w}{w_s}\right)^{3+2/\lambda} \qquad \text{(b.6)}$$

The subscript s denotes the values at saturation, and λ is a constant, which depends on the texture of the soil. For many soils, w_s has the value of 0.4 m^3 m^{-3} (Garratt, 1992). The surface heat source/sink S_{T0} is

$$S_{T0} = R_n - H_{s0} - H_{L0} \qquad \text{(b. 7)}$$

where R_n is net radiation, H_{s0} is sensible heat flux and H_{L0} is latent heat. The surface water source/sink S_{w0} obeys

$$S_{w0} = P_r - H_{L0}/L = P_r - E_0 \qquad \text{(b. 8)}$$

where P_r is precipitation rate, E_0 is evaporation rate, L is latent heat of evaporation or sublimation.

The heat fluxes are given by

$$H_{s0} = (1-\sigma_f)H_g + \sigma_f H_f \qquad \text{(b. 9)}$$

$$E_{s0} = (1-\sigma_f)E_g + \sigma_f E_f$$

The subscript g denote over the bare ground and subscript f for foliage. σ_f is the percent of the area covered by plants. The components of sensible and latent heat fluxes can be expressed by

$$H_g = -\rho c_p u_* \theta_{g*} = \rho c_p C_h |V_a|(\Theta_g - \Theta_0) = \rho c_p (\Theta_g - \Theta_0)/r_b \qquad \text{(b. 10)}$$

$$H_f = -\rho c_p u_* \theta_{f*} = \rho c_p C_h |V_a|(\Theta_f - \Theta_0) = \rho c_p (\Theta_f - \Theta_0)/r_d \qquad \text{(b. 11)}$$

$$E_g = -\rho c_p u_* q_{g*} = \rho c_p C_h |V_a|(Q_g - Q_0) = \rho (Q_g - Q_0)/r_b \qquad \text{(b. 12)}$$

$$E_f = -\rho c_p u_* q_{f*} = \rho c_p C_h |V_a|(Q_f - Q_0) = \rho (Q_f - Q_0)/(r_b + r_s) \qquad \text{(b. 13)}$$

The drag coefficient C_h can be calculated by the similarity equation (Businger *et al.*, 1971) if Θ_g, Θ_f, and Θ_0 are given. r_b is the resistance between the ground and atmosphere, and r_d is between canopy and atmosphere, and r_s is the surface resistance due to the unsaturated ground. Θ_0 and Q_0 are the average potential temperature and mixing ratio of the values for air, ground, and vegetation, as shown in Fig. 2 (Garratt, 1992). The surface resistance is calculated by

$$r_s = r_{s,min} F_1 F_2 F_3 F_4 \qquad \text{(b. 14)}$$

F_1 = the effect of photosynthetically active radiation
F_2 = the effect of soil moisture
F_3 = the effect of vapor pressure deficit
F_4 = the effect of air temperature

(b. 15)

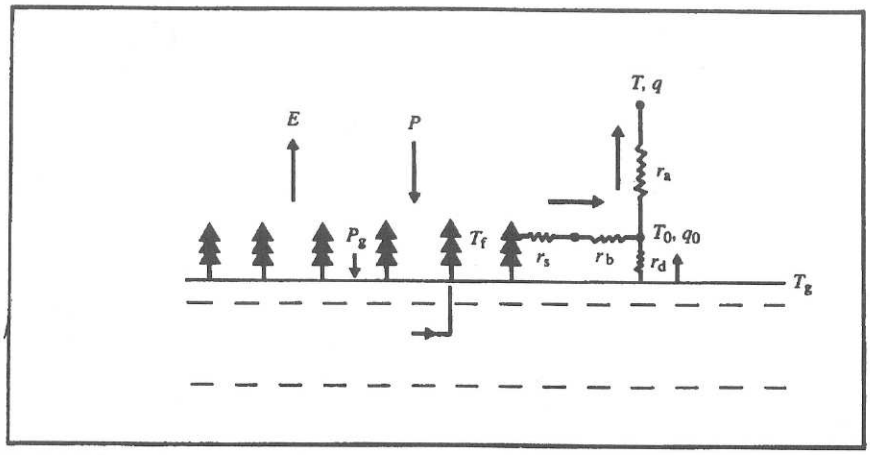


Fig. 8.9 Schematic representation of the main elements of a non-isothermal or two-component canopy model. Linked to the atmosphere (via resistances r_s, r_b and r_a), to the soil or undergrowth (via resistance r_d) and the deep soil (via evapotranspiration), the canopy and upper soil layer are at temperatures T_f and T_g. P_g is the precipitation reaching the soil surface.

In a numerical model, evaporation over the unsaturated bare ground is usually calculated by one the following three methods:

$$E_g = \rho\left(\alpha Q_s\left(T_g\right) - Q_a\right)/r_b \text{ (alpha method), or} \qquad \text{(b. 16)}$$

$$E_g = \beta\left(Q_s\left(T_g\right) - Q_a\right)/r_b \text{ (beta method), or} \qquad \text{(b. 17)}$$

$$E_g = \min\left(E_p, E_c\right) \textit{ threshold method (i.e., sup ply and demand mehtod)}$$
$$\textit{where}$$
$$\textit{potential evaporation } E_p = \left(Q_s\left(T_g\right) - Q_a\right)/r_b, \textit{ and} \qquad \text{(b. 18)}$$
$$\textit{Ec is the sup ply of the moisture flux trhough the layer benath.}$$

where E_c is the supply of moisture from the layer beneath the surface, which can be calculated by (b.4)or following Eq. (33) of Dickinson et al. (1993)

The vegetation and ground temperature are expressed by

$$C_f \frac{\partial T_f}{\partial t} = R_{nf} - H_{s0f} - H_{L0f} \qquad \text{(b. 19)}$$

$$C_g \frac{\partial T_g}{\partial t} = -\frac{\partial Q_T}{\partial z} + R_{ng} - H_{s0g} - H_{L0g} \qquad \text{(b. 20)}$$

More detailed descriptions can be found in Noilhan and Planton (1989), Garratt (1992) and LAPS model (Mihailovic *et al.*, 1992), Bosilovich and Sun (1995, 1998) and Shao *et al.* (1999).

In addition to heat and moisture fluxes in the vertical direction, a model should also consider the surface and underground runoffs, which can be very important especially over mountains.

3. RESULTS

Three different simulations will be discussed to show: (a) interaction between atmosphere and land surface, (b) the response of land surface to atmospheric forcing, and (c) sensitivity test of soil-vegetation property.

3a: Interaction between atmosphere and land surface

Figure 3 shows the time sequence of two-day vertical profiles (from surface up to 2 km) of observed and modeled virtual potential temperature (K), mixing ratio (g kg^{-1}), westerly wind U, and southerly wind V (m s^{-1}) at Wangara, Australia (Sun, 1993a, b). The Wangara Experiment (Clarke *et al.*, 1971) provided excellent two months observational data of the atmospheric planetary boundary layer (PBL) from surface up to 2 km and has been used to verify the model simulations (Deardorff, 1974; Sun and Ogura, 1980; and others). But it did not provide the property of vegetation and soil.

Figure 3a shows the vertical contributions of the TKE from buoyancy, transport, and dissipation according to (a.5). A well mixed layer with a uniformed potential temperature, mixing ratio, and wind field developed in the afternoon. But a strong temperature gradient (i.e., nocturnal inversion) and low-level jet developed at nighttime are well reproduced by the model. Figure 3b shows the contribution of surface energy (b.7). Figures 3c-d reveal observed and simulated potential temperatures and mixing ratios at and near the surface (z=0.01, 2.5, and 10 m). Overall over the model reproduces the observed features quite well.

3b: Response of soil and vegetation to atmospheric forcing

Bosilovich and Sun (1998) applied the one-dimensional Land-surface surface model to simulate the surface variables during the First ISLSCP Field Experiment (FIFE) (Sellers *et al.*, 1988; Strebel *et al.*, 1994) in 25 June-25 July 1987. The forcing from the atmosphere near the surface is shown in Fig. 5. The parameters and the set up of simulations are presented in Table 1.

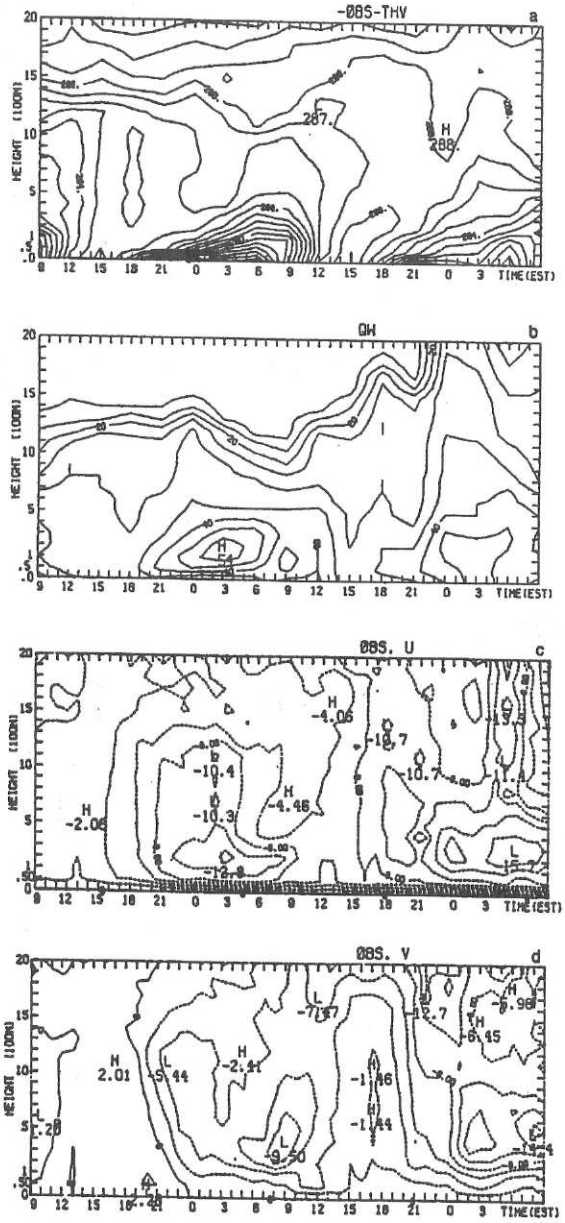


Figure 1 The time and spatial variation of measured variables from 0900 EST, Day 33 to 0900 EST: (a) Θ_v (K) (b) Q (labels scaled by 10000), (c) U ($m\ s^{-1}$), and (d) V ($m\ s^{-1}$).

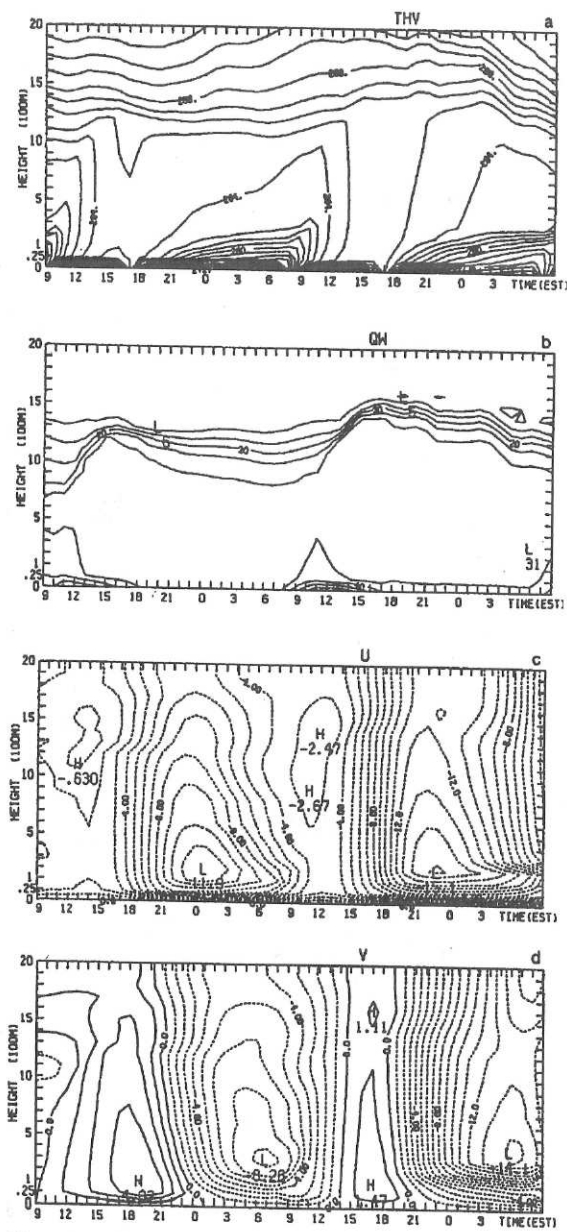


Figure 2 As Figure 1, except calculated values (a) Θ_v, (b) Q, (c) U, and (d) V.

Fig. 3. (after Sun, 1993a)

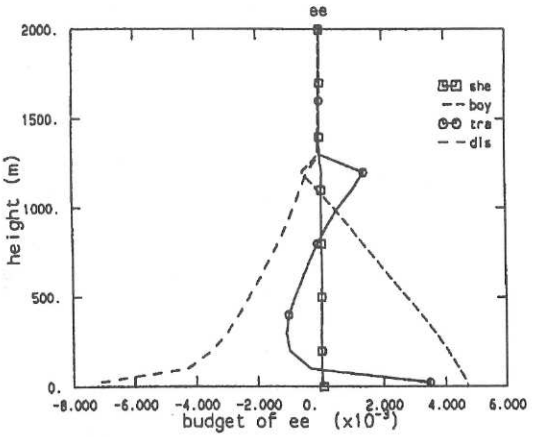


Figure 8 Contributions of the TKE budget at 1500 of Day 33 (unit: $m^2 s^{-3}$).

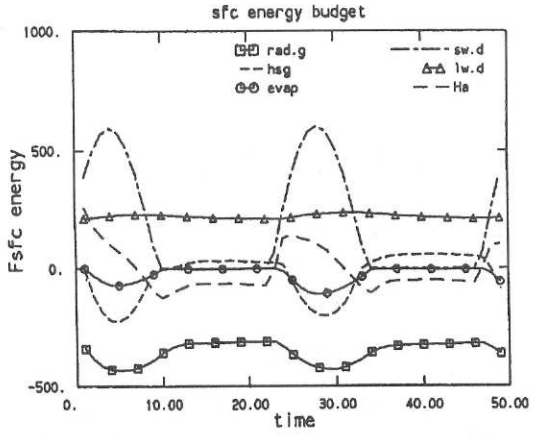


Figure 9 Contributions of surface energy budget of Eq. (2.21) (unit: $W m^{-2}$).

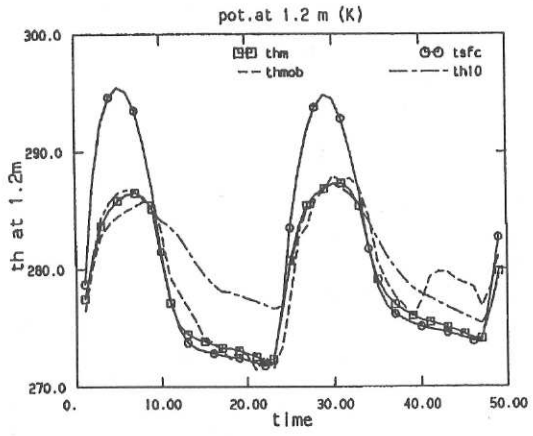


Figure 10 Θ_v measured at z = 1.2 m (thmob), and the values calculated at surface (tsfc), z = 1.2 m (thm), and z = 10 m.

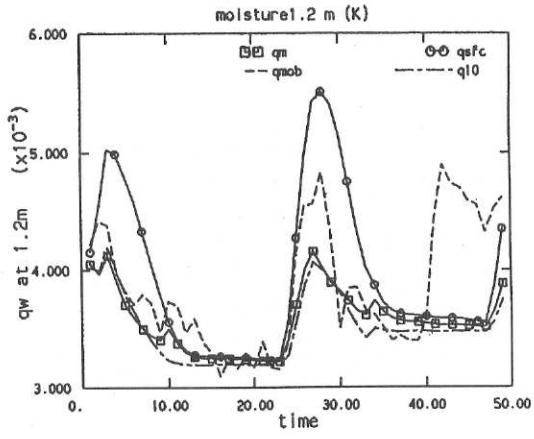


Figure 11 Q measured at z = 1.2 m (qmob), and the values calculated at surface (qsfc), z = 1.2 m (qm), and z = 10 m (q10).

Fig. 4. (after Sun, 1993a)

TABLE 1. Boundary conditions and model constants. The soil type is used to specify several constants related to the soil texture: z_{0m} is the roughness length of bare soil, ϵ_s is the emissivity of the soil surface, σ_f is the fraction of vegetation cover, h_c is the canopy height, LAI is the leaf area index, R_{smin} is the minimum stomatal resistance of the canopy, and ϵ_c is the emissivity of the vegetation canopy.

Soil type	z_{0m} (m)	ϵ_s	σ_f	h_c (m)	LAI (m^2 m^{-2})	R_{smin} (s m^{-1})	ϵ_c
Silty clay loam	0.05	0.96	0.80	0.50	1.30	125.00	0.90

TABLE 2. Soil model structure and initialization for the Bosilovich and Sun (1995) model with eight and five layers and the FRM surface and bulk layers: Z is the midpoint depth of the layer, ΔZ is the thickness of the soil layer, w is the initial volumetric soil water content, T is the initial soil temperature, λ is the soil thermal conductivity, and c_{ro} is the root fraction. Note that for the FRM Z and ΔZ are for the soil moisture prediction equation, the soil temperature equations use variable thicknesses.

Layer	Z (m)	ΔZ	w ($m^3 m^{-3}$)	T (K)	λ (W m^{-1} K^{-1})	C_{ro}
1	0.005	0.01	0.357	289.0	1.1	0.00
2	0.020	0.02	0.357	290.0	1.1	0.00
3	0.050	0.04	0.352	293.0	1.1	0.15
4	0.100	0.06	0.360	296.0	0.6	0.30
5	0.200	0.14	0.370	296.0	0.2	0.30
6	0.500	0.46	0.370	295.2	0.2	0.25
7	0.990	0.52	0.370	295.2	0.2	0.00
8	1.625	0.75	0.380	295.2	0.2	0.00
1	0.025	0.05	0.350	290.0	1.1	0.10
2	0.175	0.25	0.370	295.2	0.2	0.70
3	0.500	0.40	0.370	295.2	0.2	0.20
4	1.000	0.60	0.370	295.2	0.2	0.00
5	1.650	0.70	0.380	295.2	0.2	0.00
			FRM			
1	0.05	0.10	0.370	288	1.1	0.20
2	1.000	2.00	0.370	295.2	0.2	0.80

TABLE 3. Description and differences for each model simulation presented in this paper. All simulations use the vegetation model and beta method, unless noted otherwise.

Case	Description
1	Eight soil layers, Beta moisture availability
2	Five soil layers, Beta moisture availability
3	Eight soil layers, Alpha moisture availability
4a	Force–Restore Method, Deardorff (1978) C_g and C_t
4b	Force–Restore Method, Braud et al. (1993) C_g and C_t
5a	Eight soil layers, no vegetation model
5b	FRM Deardorff (1978), no vegetation model
5c	FRM Braud et al. (1993), no vegetation model

TABLE 4. Rms error and bias (in parentheses) of model surface and 50-cm soil temperature. Note that observed surface temperature is measured by a radiometer and 50-cm soil temperature is a point observation. Units are kelvin.

Case	T surface	T at 50 cm
1	0.94 (0.83)	0.20 (0.03)
2	0.79 (0.52)	0.33 (−0.16)
3	1.14 (1.02)	0.23 (0.19)
4a	1.04 (0.93)	0.94 (0.78)
4b	0.90 (0.63)	0.61 (0.51)
5a	1.14 (0.73)	0.37 (0.35)
5b	1.84 (1.54)	1.72 (1.70)
5c	1.12 (0.02)	0.92 (0.89)

Table 1. (after Bosilovich and Sun, 1998)

The observed and simulated surface and 50-cm soil temperature are shown in Figs. 6 and 7. We can see that the observed temperature and moisture at surface and inside the soil are well reproduced; we can also see that the magnitude of E_f is comparable to E_g in Fig. 7. It is also noted that there is larger soil water content and less evaporation for the alpha method (b.16) compared to the beta method (b.17) when the soil moisture is less than field capacity, which will be discussed later. The results shown here are calculated based on beta method with eight soil layers. More detailed discussion is referred to Bosilovich and Sun (1998).

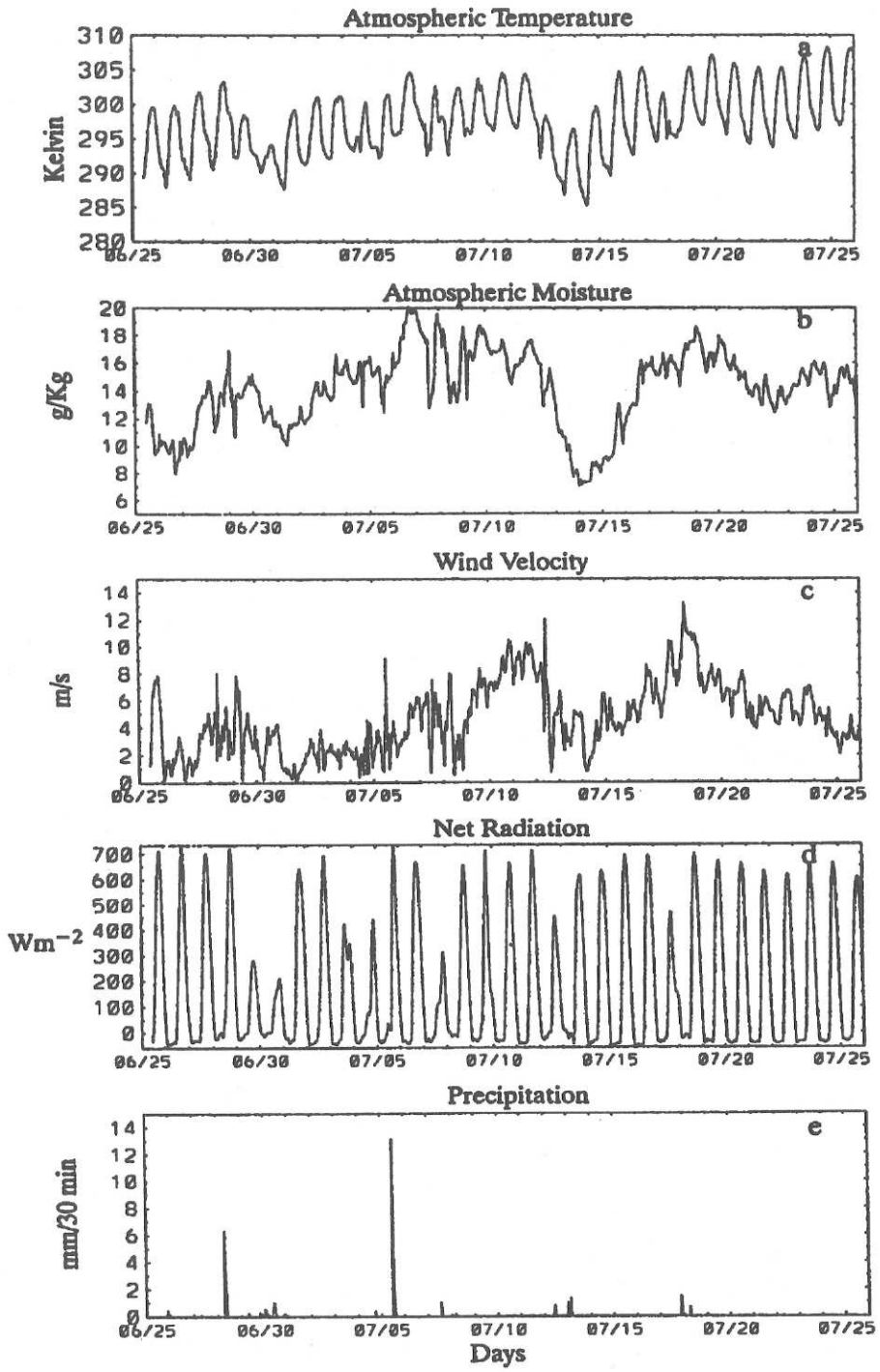


FIG. 1. FIFE site average data used as input to the model: (a) 2.0-m atmospheric temperature, (b) 2.0-m atmospheric specific humidity, (c) 5.4-m wind speed, (d) surface net radiation (computed from component radiative fluxes), and (e) precipitation rate.

Fig. 5. (after Bosilovich and Sun, 1998)

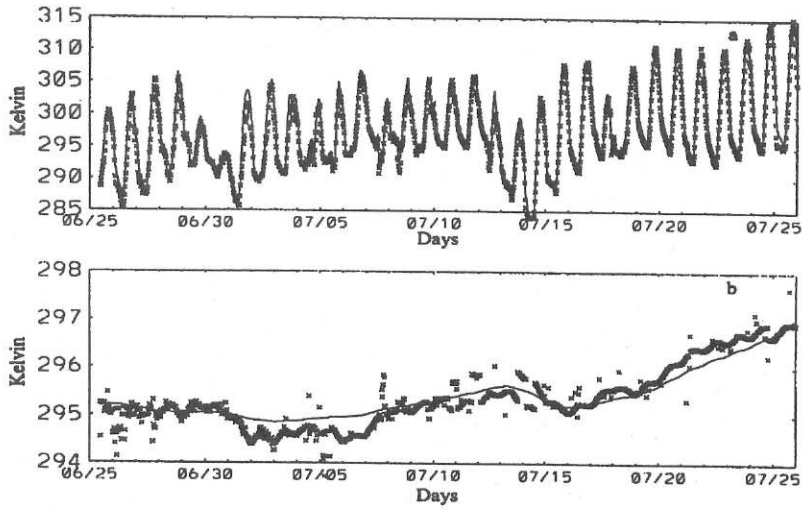


FIG. 2. Time series comparison of model-simulated (case 1) (a) surface temperature and (b) 50-cm soil temperature (solid line represents model data and crosses are observations).

Fig. 6. (after Bosilovich and Sun, 1998)

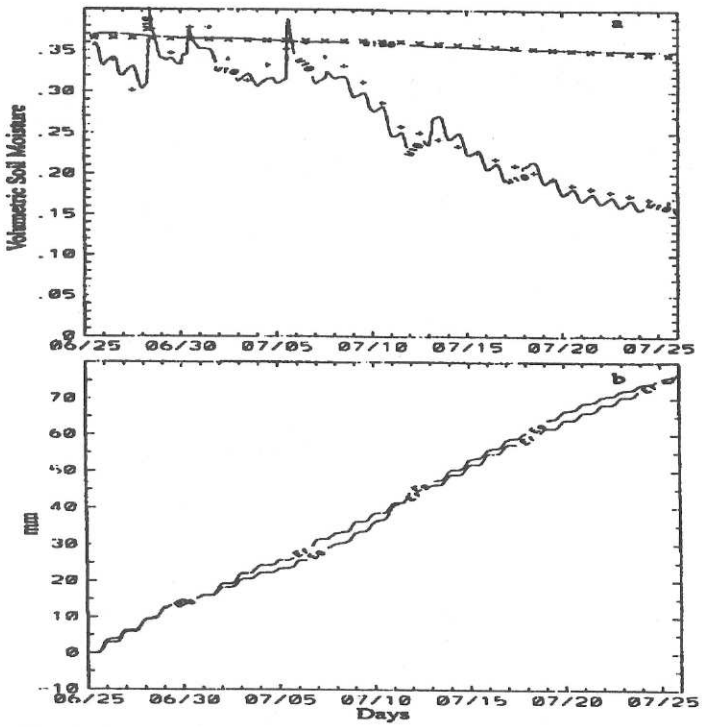


FIG. 3. Case 1 (a) comparison of model and observed soil moisture, and (b) model-simulated cumulative evaporation for the ground surface (E_g) and vegetation surface (E_f): (+) indicates observed gravimetric soil moisture for the layer 0–10 cm, and (×) indicates the neutron probe soil moisture observations at 1 m. The line marked W10 is the model 0–10-cm soil water content, and W100 is the soil water content of the layer centered at 1 m.

Fig. 7. (after Bosilovich and Sun, 1998)

3c: Sensitivity test of soil-vegetation property

Sun and Bosilovich (1996) applied the one-dimensional atmospheric model (Sun, 1993a, b) and land-surface package to study the response of turbulence fluxes and atmospheric profiles to the variation of vegetation cover, minimum stomatal resistance, canopy height, initial soil moisture, and soil type. The model set up and parameters are shown in Tables 2. The leave area index (LAI)=5.5 and simulation is from 00Z to 12Z). We will present the results due to the variation of soil moisture, minimum stomatal resistance and vegetation coverage, and soil type.

Table I

Soil model initial conditions and grid spacing. Δz is the thickness of the soil layer. The initial soil temperature for layers 2–5 was derived for the observational data set. Soil moisture was initialized from a 'stand alone' simulation (Bosilovich and Sun, 1995). The root distribution is used to compute root zone soil moisture, and determines the percentage of transpiration that is removed from a layer

Layer	Δz (cm)	T (K)	W (m^3 m^{-3})	Root Dist. (%)
1	1	291.00	0.195	5
2	2	291.00	0.195	10
3	10	292.75	0.210	30
4	14	293.25	0.215	30
5	26	294.00	0.225	25
6	47	294.00	0.235	0

Table II

Table of variables used in the sensitivity study. Boldface indicates the sensitivity variable and its range in the simulations. σ_f' is the percentage of leaf area to ground area, 100% implies complete coverage of the ground. r_{smin} is the minimum stomatal resistance. h_{can} is the height of the canopy. W_U and W_L are the initial soil moistures of the upper three and lower three soil layers respectively, in units of volumetric soil water

Experiment	σ_f' (%)	r_{smin} (sm^{-1})	h_{can} (m)	W_U, W_L	Soil type
1a	**0–100**	50	0.50	0.13, 0.19	Loam
1b*	**0–100**	50	0.50	0.13, 0.19	Loam
2a	70	**25–525**	0.50	0.13, 0.19	Loam
2b	**0–100**	500	0.50	0.13, 0.19	Loam
3	75	50	**0.01–2.0****	0.13, 0.19	Loam
4a	0	–	0.50	**0.04–0.24**†	Loam
4b	75	50	0.50	**0.04–0.24**†	Loam
5a	0	–	0.50	0.18, 0.22	**Sand–Clay**
5b	75	50	0.50	0.18, 0.22	**Sand–Clay**
5c	0	–	0.50	‡	**Sand–Clay**
5d	75	50	0.50	‡	**Sand–Clay**

*Experiment 1b is identical to 1a, except that the Force Restore Method is used.
** The canopy height is varied logarithmically.
† The range of upper soil layers is provided, the lower soil layers range is 0.09–0.29.
‡ Soil moisture also varies for this experiment (see text).

Table 2. (after Sun and Bosilovich, 1996)

Experiment of vegetation

Evapotranspiration is strongly affected by the stomatal resistance, according to (b.13)-(b.15). The stomata are pores which, when open, are the main conduits for transpired water. Hence, the net resistance r_s to water passing from the inside to the outside of the leaf depends largely on the size, distribution, and degree of opening of those stomata. The value of minimum stomatal resistance is from 30-40 s m^{-1} (crops and grassland) to 200-300 s m^{-1} for citrus according to Garratt (1992; Table 5-1); the values are from 25 to 300 s m^{-1} for crops and grasses and 500-2000 s m^{-1} for trees according to Monteith (1976); the range is 120-200 s m^{-1} according to Dickinson *et al.*(1993, Table 2). Hence, the values are uncertain.

The vertical profiles of virtual potential temperature, mixing ratio, and TKE as function of minimum stomatal resistance are shown in Fig. 8 (Experiment 2a). The higher (lower) the resistance, the less (more) water substance is permitted to the leave the plant. Hence, the depth of the PBL is higher and PBL is drier for a smaller value of resistance. However, when the minimum resistance is very high (here is 500), Figure 9 shows the vegetation under a stressed condition can become an effective barrier for surface moisture flux. (Experiment 2b).

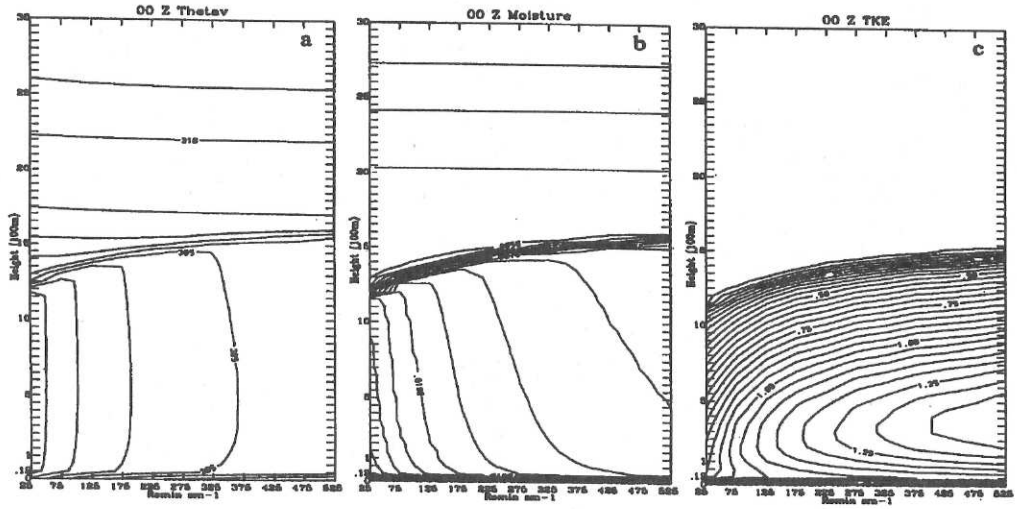


Figure 6. **Sensitivity Experiment 2a. 0000 Z vertical profiles of (a) virtual potential temperature (1 K interval), (b) specific humidity (0.5 × 10^{-3} Kg/Kg interval), and (c) TKE (0.05 m^2 s^{-2} interval). Minimum stomatal resistance is the sensitivity variable.**

Fig. 8 (after Sun and Bosilovich, 1996)

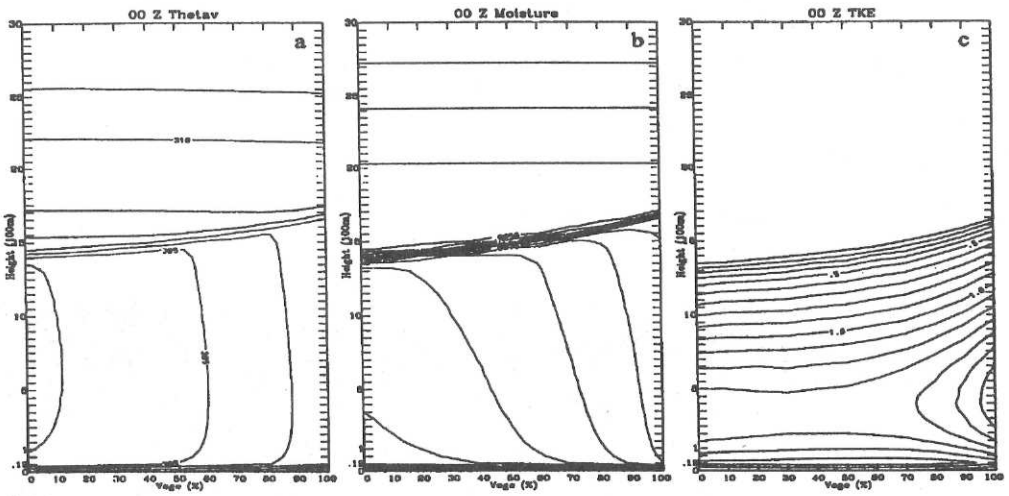


Figure 7. As in Figure 6, except for Sensitivity Experiment 2b, where the sensitivity variable is the vegetation cover. The contour intervals are identical to Figure 6.

Fig. 9. (after Sun and Bosilovich 1996)

Experiment of initial soil moisture

The important factors to determine evaporation rate from bare soil are field capacity and wilting point, they are dependent on soil texture, as shown in Fig. 12.

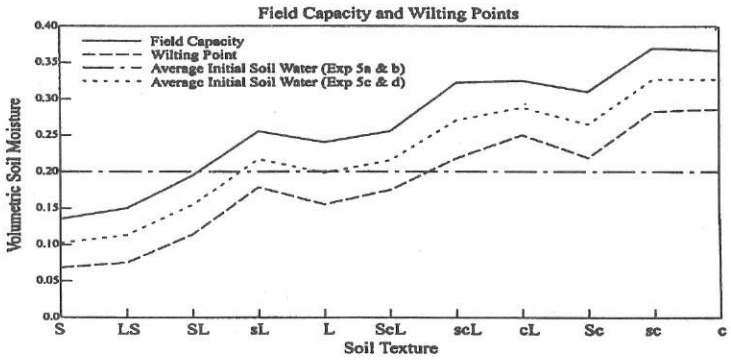


Figure 13. Comparison of the wilting points and field capacities for given soil textures to the initial soil water content used in Experiment 5. Soil textures are abbreviated by the following: S = sand(y), s = silt(y), L = Loam(y), and c = clay. Example: ScL = Sandy clay loam.

Fig. 10. (after Sun and Bosilovich, 1996)

The evaporation occurs at potential rate (moisture availability is 100%) when soil moisture is greater than the field capacity, but evaporation shots down when soil moisture is less than wilting point.

Figures 11a-b show the surface sensible and latent heat fluxes as function of initial upper soil moisture and time.

Figures 11c-e show the vertical profiles of potential temperature, mixing ratio, and TKE as function of upper layer soil moisture without vegetation. Over a wet soil, the PBL is cooler and more moist, and the depth of PBL is lower depth compared with that developed over a dry land.

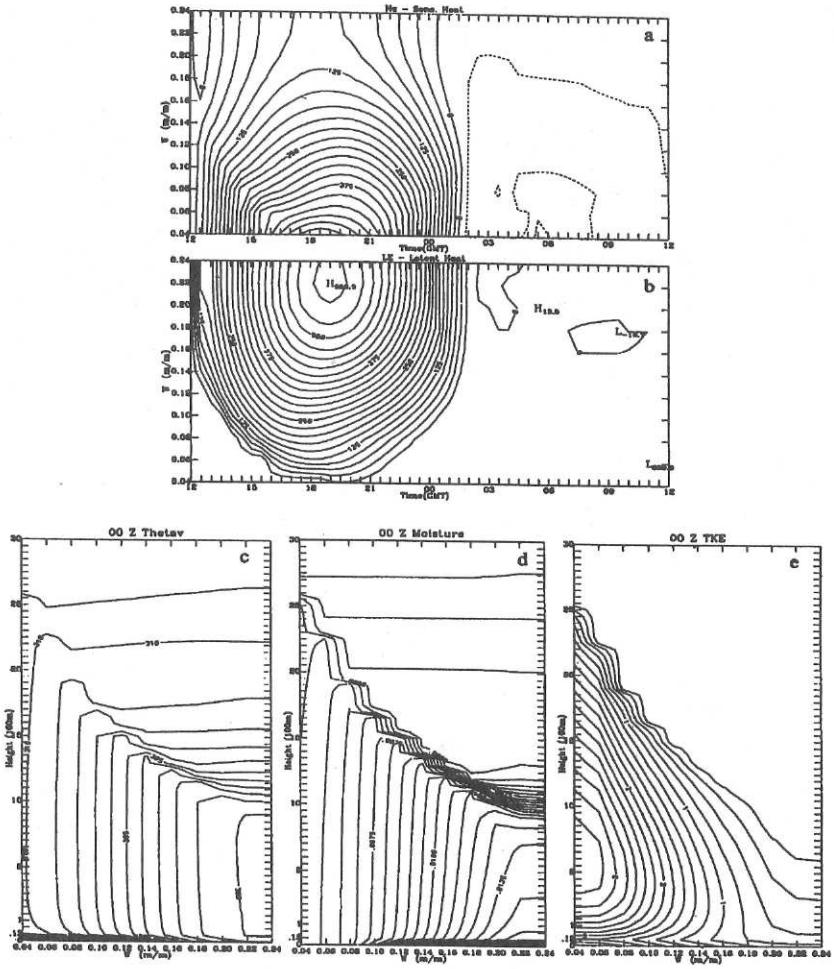


Figure 10. As in Figure 4, except for Sensitivity Experiment 4a, where the initial soil water content is the sensitivity variable. The contour intervals are identical to Figure 4 for all, except TKE ($0.25\ m^2\ s^{-2}$).

Fig. 11. For bare ground (after Sun and Bosilovich, 1996)

Figures 12a-b show ground surface temperature and vegetation temperature for Experiment 4b. The vertical profiles of potential temperature, mixing ratio, and TKE as function of upper layer soil moisture are shown in Fig. 12c-e (with 75% vegetation cover and r_s =50 s m^{-1}). The variation for small value of soil moisture is quite large, but variation becomes small for soil moisture > 0.14, when it is greater than

field capacity. The moisture can free be transported through the atmosphere by both bare ground and vegetation. It is also noted that vegetation with small resistance can effectively transfer the soil moisture from root zone into the atmosphere under normal condition.

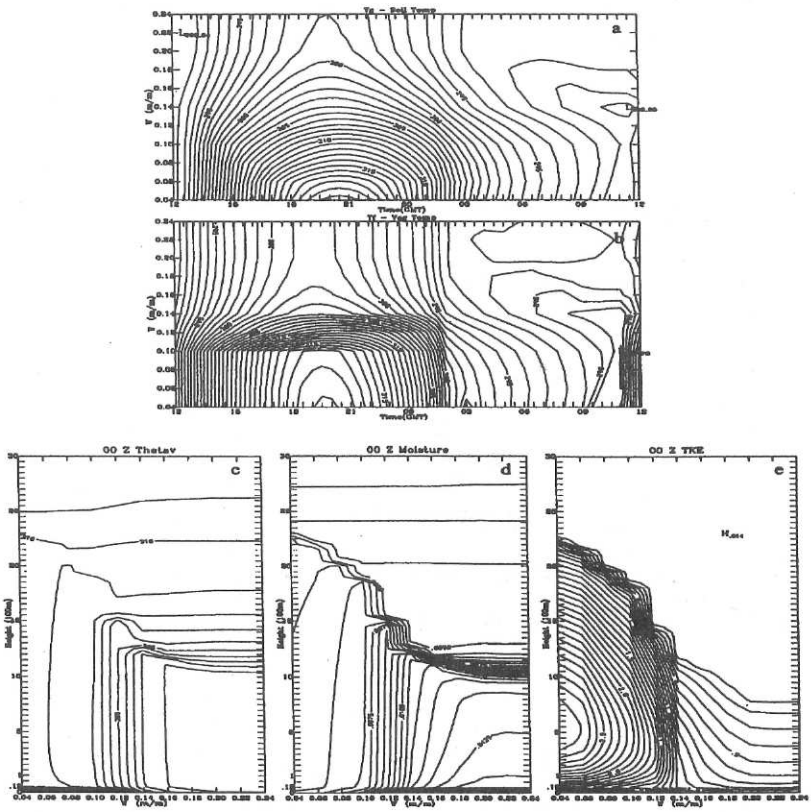


Figure 11. **Sensitivity Experiment 4b, same as Experiment 4a except vegetation is included. (a) Ground surface temperature and (b) vegetation surface temperature, both at a contour interval of 1 K. Comparison of 0000 Z vertical profiles of (c) virtual potential temperature (1 K interval), (d) specific humidity (0.5×10^{-3} Kg/Kg interval), and (e) turbulent kinetic energy ($0.10\ m^2\ s^{-2}$ interval). Initial soil water content is the sensitivity variable.**

Fig. 12. With 75% vegetation coverage(after Sun and Bosilovich, 1996)

4. Summary

The equations and numerical results of atmosphere-vegetation-soil interaction are briefly presented here. Observational data are very limited, numerical model becomes the major tool in this area. The models presented here seem be able to reproduce many major features of observations. The models also provide plausible explanation of mechanisms involved. However, more observations are required to verify both equations and the parameters involved. It also requires scientists in different disciplines to work together to study the complex processes at and near the ground

surface, where the human beings depend on. After we have a better understanding of those processes, we may be able to develop a better planning of the land usage as well as to predict the change of regional climate, water resources, and ecological system.

5.REFERENCES

Beljaars, A. C. M., P. Viterbo, M. J. Miller and A. K. Betts. 1996. The anomalous rainfall over the United States during July 1993: Sensitivity to land surface parameterizations and soil moisture anomalies. *Mon. Wea. Rev.* 124: 362–383.

Betts, A. K. and J. H. Ball. 1998. FIFE surface climate and site-averaged data set: 1987–1989. *J. Atmos. Sci.* 55: 1091–1108.

Betts, A. K. and A. C. M. Beljaars. 1993. Comparison between the land surface response of the ECMWF model and the FIFE 1987 data. *Quart. J. Roy. Meteor. Soc.* 119: 975–1001.

Bhumralkar, C. M. 1975. Numerical experiments on the computation of ground surface temperature in an atmospheric general circulation model. *J. Appl. Meteor.* 14: 1246–1258.

Bosilovich, M. G. and W.-Y. Sun. 1995. Formulation and verification of a land surface parameterization for atmospheric models. *Bound.-Layer Meteor.* 73: 321–341.

Bosilovich, M. B. and W. Y. Sun. 1998: Simulation of soil moisture and temperature. *J. Atmos. Sci. 55*: 1170-1183.

Bosilovich, M. G. and W.-Y. Sun. 1999. Numerical simulation of the 1993 Midwestern Flood: Local and remote sources of water. *J. Geophys. Res. 104*: D16, 19: 415-19,423.

Bosilovich, M. G. and W.-Y. Sun. 1999. Numerical simulation of the 1993 Midwestern flood: Land-Atmosphere Interactions. *J. Climate 12*: 1490-1505.

Businger, J. A., J. C. Wyngaard, Y. Izumi and E. F. Bradley. 1971. Flux profile relationships in the atmospheric surface layer. *J. Atmos. Sci.* 28: 181–189.

Clapp, R. B. and G. M. Hornberger. 1978. Empirical equations for some soil hydraulic properties. *Water Resour. Res.* 14: 601–604.

Deardorff, J. W. 1977. A parameterization of the ground surface moisture content for use in atmospheric prediction models. *J. Appl. Meteor.* 16: 1182–1185.

Deardorff, J. W. 1978. Efficient prediction of ground surface temperature and moisture with inclusion of a layer of vegetation. *J. Geophys. Res.* 83: 1889–1903.

Dickinson, R. E. 1984. Modeling evapotranspiration for three-dimensional global climate models. *Climate Processes and Climate*

Sensitivity, Geophys. Monogr. 29: 58–72.

Dickinson, R. E. 1988. The force restore model for surface temperatures and its generalizations. *J. Climate* 1: 1086–1097.

Dickinson, R. E. A. Henderson-Sellers and P. J. Kennedy. 1993. Biosphere-Atmsophere Transfer Scheme (BATS) Version 1e as Coupled to NCAR Community Climate Model, NCAR Technical Note, NCAR/TN-387+STR, 72 pp.

Garratt, J. R. 1992. The atmospheric boundary layer. Cambridge University Press. 316pp.

Manabe, S. 1969. The atmospheric circulation and the hydrology of the earth's surface. *Mon. Wea. Rev.* 97: 739–774.

Mihailovic, D., H. A. R. de Bruin, M. Jeftic and A. van Dijken. 1992. A study of the sensitivity of land surface parameterizations to the inclusion of different fractional covers and soil textures. *J. Appl. Meteor.* 31: 1477–1487.

Noilhan, J. and S. Planton. 1989. A simple parameterization of land surface processes for meteorological models. *Mon. Wea. Rev.* 117: 536–549.

Philip, J. R. 1957. Evaporation, and moisture and heat fields in the soil. *J. Meteor.* 14: 354–366.

Sellers, P. J, F. G. Hall, G. Asrar, D. E. Strebel and R. E. Murphy. 1988. The First ISLSCP Field Experiment (FIFE). *Bull. Amer. Meteor. Soc.* 69: 22–27.

Shao, Y., R. D. Anne, A. Henderson- Sellers, P. Irannejad, P. Thornton, X. Liang, T. H. Chen, C. Ciret, C. Desborough, O. Balachova, A. Haxeltine and A. ducharne. 1999. Soil moisture simulation- A report of the RICE and PILPS Workshop. http:/cic.mq.edu.au/pilps-rice/publication/soilm/WkSp-Rep3.htlm

Strebel, D. E., D. R. Landis, K. F. Huemmrich and B. W. Meeson. 1994. *Collected Data of the First ISLSCP Field Experiment. Vol. 1, Surface Observations and Non Image Data Sets.* NASA, CD-ROM.

Sun, W.-Y. and J.-D. Chern. 1993. Diurnal variation of lee vortices in Taiwan and surrounding area. *J. Atmos. Sci.* 50: 3404–3430.

Sun, W.-Y. and M. G. Bosilovich. 1996. Planetary boundary and surface layer sensitivity to land surface parameters. *Bound.-Layer Meteor.* 77: 353–378.

Sun, W. Y., M. G. Bosilovich and J. D. Chern. 1997. CCM1 regional response to anomalous surface properties. *Terrestrial, Atmospheric and Oceanic Sciences 8:* 271-288.

Sun, W. Y. and J. D. Chern. 1994: Numerical experiments of vortices in the wake of idealized large mountains. *J. Atmos. Sci. 51*: 191-209.

Sun, W. Y. 1993a. Numerical simulation of a planetary boundary layer: Part I. Cloud-free case. *Beitrage zur Physik der*

Atmosphare 66: 3-16.

Sun, W. Y. 1993b. Numerical simulation of a planetary boundary layer: Part II. Cloudy case. *Beitrage zur Physik der Atmosphare 66:* 17-30.

Sun, W. Y. 1988. Air pollution in a convective atmosphere. Library of Environmental Control Technology (ed. Cheremisinoff. Gulf Publishing). p.515-546.

Sun, W. Y. and Y. Ogura. 1980. Modeling the evolution of the convective planetary boundary layer. *J. Atmos. Sci. 37:* 1558-1572.

Wu, C.-C. and W. Y. Sun. 1990. Diurnal oscillation of convective boundary layer. Part I: Cloud-free Atmosphere. *Terrestrial, Atmospheric and Oceanic Sciences 1:* 23-43.

Wu, C.-C. and W. Y. Sun. 1990. Diurnal oscillation of convective boundary layer. Part II: Cloudy Atmosphere. *Terrestrial, Atmospheric and Oceanic Sciences 2:* 157-174.

第六章　空氣、土壤及植物之交互作用

商文義

美國普度大學地球及大氣科學系

摘　要

從空氣、土壤及植物之基本流力方程式，我們在普度大學發展一套「空氣、土壤及植物交互作用」的數學模式。這個模式能夠模擬地面及地表附近所觀測的一些重要現象，同時幫助我們瞭解其中的物理現象。然而，很明顯地，我們仍需要收集更多的觀測資料，並鼓勵更多不同領域的科學家共同來探討這些物理機制，才可能發展一套完整的數值模式來預測爲來氣候、水資源及生態的變化。

關鍵詞：基本公式、潛在溫度、混合率、Richards' equation、Darcy-buckingham equation、物質潛勢、水分傳導係數、阻力、最低氣孔阻力、植冠高度、葉面積指數、PBL、植冠覆蓋、凋萎點、田間容水量、表面能量預算、表面水分預算、Stand alone model、土壤結構、土壤水分。